ISSN: 2277-9655
Impact Factor: 4.116

IJESRT

INTERNATIONAL JOURNAL OF ENGINEERING SCIENCES &RESEARCH TECHNOLOGY

THEORICAL STUDY OF INTERNAL QUANTUM EFFICIENCY BASED ON HOMOJONCTION $CuInSe_2$ (n/p) WITH CDS WINDOW GROWN ON CDTE SUBSTRATE

C.Sow, B.Mbow, Y.Tabar, B.Ndiaye, M.Thiam, E.M. Keita

Laboratoire des Semiconducteurs et d'Energie Solaire,Département de Physique,Faculté des Sciences et Techniques,Université Cheikh Anta Diop ,Dakar,Sénégal

DOI: 10.5281/zenodo.233434

ABSTRACT

The main objective of this work is to do a comparative study of the spectral responses of three models: homojunction $CuInSe_2$ with CdS window layer (CdS (n) / $CuInSe_2$ (n) / $CuInSe_2$ (p)), homojunction $CuInSe_2$ deposited on CdTe substrate ($CuInSe_2$ (n) / $CuInSe_2$ (p) / CdTe (p)) and homojunction $CuInSe_2$ with a window layer (CdS) and deposited on a CdTe substrate (P) / CdTe (p) :CdS (n) / $CuInSe_2$ (n) $CuInSe_2$ (p)/CdTe (p). We calculated the expressions of these respective spectral responses by solving the continuity equations governing the variation of the minority carriers in each region for each model and using the appropriate boundary conditions. We made a simulation of intern quantum efficiency according to the energy of the photons while preserving the same values of geometrical parameters .The results show that the homojunction with window and deposited on a substrate (CdS (n) / $CuInSe_2$ (n) $CuInSe_2$ (p) / CdTe (p) gives the best internal quantum efficiency. The window layer reduces the losses at the surface at the window-emitter interface. The substrate increases the collection of the carriers in the base. After choosing the best model, we studied the influence of geometrical and electrical parameters on the spectral response. We have also seen that the best spectral response is obtained with a small thickness of the emitter, a diffusion length of the holes and electrons respectively greater than the thickness of the buffer layer and the absorbing layer.

KEYWORDS:Spectral Response ,Window Layer , Substrate ,Solar Cells ,Homojonction, CdS ,$CuInSe_2$,CdTe.

INTRODUCTION

$CuInSe_2$ is a ternary compound of type I-III-VI_2 which has presented growing interest in recent years [1]. It is a promising material of the absorbing thin layers of the photovoltaic cells. Its bandwidth varies between 0.6 and 1.08 eV [2] and is well suited for photovoltaic conversion. The main advantages of this semiconductor material under its chalcopyrite structure are as follows [3]: a direct gap with a value of 1.04 eV; an absorption coefficient is very high in the visible and near infrared domains.;a layer of $CuInSe_2$ with a thickness of 1 µm allows the absorption of 99% of the photons arriving at the surface of the cell . To reach this same rate of absorption in the case of the silicon cells it use a thickness of approximately of 300µm.This material has good lattice matched with the CdS and CdTe layers. In order to improve the internal quantum efficiency we will do a comparative study of three photopile models: a $CuInSe_2$ homojunction with CdS window layer: (CdS (n) / $CuInSe_2$ (n) / $CuInSe_2$ (p) , $CuInSe_2$ homojunction deposited on a CdTe substrate ($CuInSe_2$ (n) / $CuInSe_2$ (p) / CdTe (p)) , and a $CuInSe_2$ homojunction with a window layer (CdS) And deposited on a CdTe substrate (CdS (n) / $CuInSe_2$ (n) / $CuInSe_2$ (p) / CdTe (p).The substrate will have the function to return the carriers no collected to the space charge region so that they take part in the photocurrent.

ISSN: 2277-9655
Impact Factor: 4.116

MATERIALS AND METHODS

1.Presentation of the layers

In this work, the materials used are $CuInSe_2$,CdTe et CdS . The properties are given in Table 1. The choice of these materials is based on the absorption coefficients , Gap energies, electronic affinities.

Matériaux	Gap energies (eV)	a (Å)	c (Å)	electronic affinities (eV)	Références
$CuInSe_2$ (p, n)	0,96 – 1 ,04	5,78	11 ,62	4,58	[5]
CdTe (p)	1,5 ±0,01	6,481	--	4,28	[6]
CdS (n)	2,4	4,1381	6,7157	4,5	[7]

Table 1: the different physical parameters used in this word

2. Theoretical study

2.1. Homojunction with window layer CdS (n) / $CuInSe_2$ (n) / $CuInSe_2$ (p)

2.1.1. Modeling

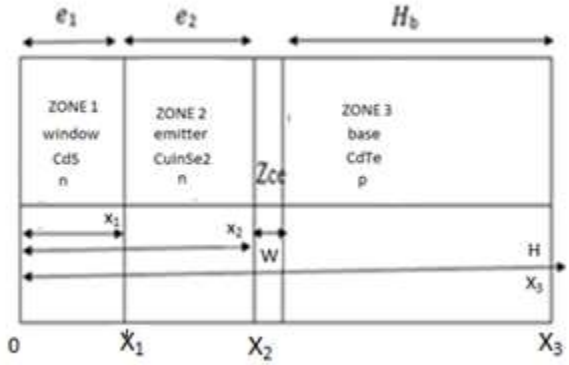

Fig 1 Diagram of the structure CdS (n)/$CuInSe_2$ (n)/ $CuInSe_2$ (p)

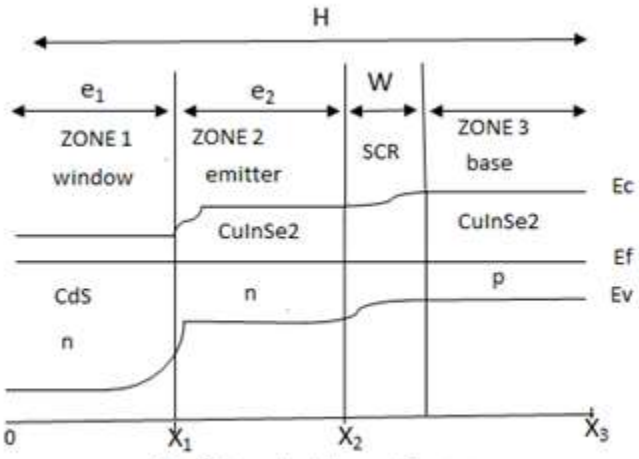

Fig 2 Energy band diagram of the structure CdS(n)/$CuInSe_2$(n)/$CuInSe_2$(p)

2.1.2. Internal quantum efficiency of the window layer (zone1)

The differential equation governing the variation of the holes in the window of type (n) in static mode [8] is

$$\frac{\partial^2 \Delta p_1}{\partial^2 x} - \frac{\Delta p_1}{Lp_1^2} + \frac{\alpha_1 N(1-R)e^{-\alpha_1 x}}{Dp_1} = 0 \qquad (1)$$

$L_{p1}\, is$ the diffusion length of the holes in the zone1, α_1 absorption coefficient of CdS , D_{p1} the diffusion coefficient of holes in zone1, τ_{p1} lifetime of holes, N (λ) incident photon number, R (λ) reflection coefficient, E (λ) photon energy .

The following boundary conditions [8]

$$\begin{cases} \frac{\partial \Delta p_1}{\partial x} = Sp_1 \Delta p_1 & x = 0 \\ \Delta p_1 = 0 & x = x_1 \end{cases} \qquad (2)$$

Sp_1 is the surface recombination velocity of window layer.

The expression of internal quantum efficiency in the window layer is given by (zone1)

$$\eta p_1 = \frac{\alpha_1 Lp_1}{\alpha_1^2 Lp_1^2 - 1}\left[-\alpha_1 Lp_1 e^{-\alpha_1 x_1} + \frac{\left(\alpha_1 Lp_1 + \frac{Sp_1 Lp_1}{Dp_1}\right) - \left(\frac{Sp_1 Lp_1}{Dp_1}\cosh\left(\frac{x_1}{Lp_1}\right) + \sinh\left(\frac{x_1}{Lp_1}\right)\right)e^{-\alpha_1 x_1}}{\frac{Sp_1 Lp_1}{Dp_1}\sinh\left(\frac{x_1}{Lp_1}\right) + \cosh\left(\frac{x_1}{Lp_1}\right)}\right] \quad (3)$$

2.1.3. Internal quantum efficiency of the emitter layer (zone 2)

The continuity equation governing the variation of holes in the buffer layer [6] is given by:

$$\frac{\partial^2 \Delta p_2}{\partial^2 x} - \frac{\Delta p_2}{Lp_2^2} + \frac{\alpha_2 N(1-R)e^{-\alpha_1 x_1} e^{-\alpha_2 (x_2 - x_1)}}{Dp_2} = 0 \quad (4)$$

α_2 is the absorption Coefficient o $CuInSe_2$, Lp_2 is the diffusion length of the holes in the zone2 , D_{p2}: diffusion coefficient of the holes in the zone2, $e_2 = x_2 - x_1$ thickness of emitter, x_1 *is* thickness window layer .

We use the boundary conditions [5]

$$\begin{cases} Dp_2 \dfrac{\partial \Delta p_2}{\partial x} = Sp_2 \Delta p_2 + Dp_1 \dfrac{\partial \Delta p_1}{\partial x} & x = x_1 \\ \Delta p_2 = 0 & x = x_2 \end{cases} \quad (5)$$

The internal quantum efficiency is:

$$\eta p_2 = \frac{\alpha_2 Lp_2 e^{-x_1(\alpha_1 - \alpha_2)}}{\alpha_2^2 Lp_2^2 - 1}\left[-\alpha_2 Lp_2 e^{-x_2 \alpha_2} - Z\right] + \frac{\eta p_1}{\frac{Sp_2 Lp_2}{Dp_2}\sinh\left(\frac{x_2 - x_1}{Lp_2}\right) + \cosh\left(\frac{x_2 - x_1}{Lp_2}\right)} \quad (6)$$

With $$Z = \frac{\left(\alpha_2 Lp_2 + \frac{Sp_2 Lp_2}{Dp_2}\right)e^{-x_1 \alpha_2} - \left(\frac{Sp_2 Lp_2}{Dp_2}\cosh\left(\frac{x_2 - x_1}{Lp_2}\right) + \sinh\left(\frac{x_2 - x_1}{Lp_2}\right)\right)e^{-x_2 \alpha_2}}{\frac{Sp_2 Lp_2}{Dp_2}\sinh\left(\frac{x_2 - x_1}{Lp_2}\right) + \cosh\left(\frac{x_2 - x_1}{Lp_2}\right)}$$

2.1.4. Internal quantum efficiency in the space charge zone

The following differential equations allow us to calculate the internal quantum efficiency in the space charge zone [9]

$$\eta_{zce1'} = e^{-\alpha_1 x_1} e^{\alpha_2 (x_2 - x_1)}(1 - e^{-\alpha_2 w_1}) \quad [5] \quad (7)$$

$$\eta_{zce1''} = e^{-\alpha_1 x_1} e^{\alpha_2 ((x_2 + w_1) - x_1)}(1 - e^{-\alpha_3 w_2}) \quad [5] \quad (8)$$

$$\eta_{zce1} = \eta_{zce1'} + \eta_{zce1''} \quad (9)$$

2.1.5. Internal quantum efficiency of the base (zone 3)

The continuity equation governing the variation of electron in the base [10]

$$\frac{\partial^2 \Delta p_3}{\partial^2 x} - \frac{\Delta p_3}{Lp_3^2} + \frac{\alpha_3 N(1-R)e^{-x_1(\alpha_1 - \alpha_2)} e^{(x_2 + w)(\alpha_2 - \alpha_3)} e^{-\alpha_3 x}}{Dp_3} = 0 \quad (10)$$

α_3 is the absorption coefficient of $CuInSe_2$, Ln_3 *the* diffusion length of the electrons in the base des electrons, D_{n3} the diffusion coefficient of electrons, $W = W_1 + W_2$ *is the* thickness of space charge region .The boundary condition are given by [9].

$$\begin{cases} \Delta n_3 = 0 & x = x_2 + w_1 + w_2 \\ \dfrac{\partial \Delta n_3}{\partial x} = -Sn_3 \Delta n_3 & x = H \end{cases} \quad (11)$$

Sn_3 is the surface recombination velocity, H *is the* thickness of the structure, $H_b = H - (x_2 + w)$ thickness of the base (zone3).The internal quanum efficiency is given by:

$$\eta n_3 = \frac{\alpha_3 Lp_3}{\alpha_3^2 Lp_3^2 - 1} e^{x_1(\alpha_2-\alpha_1)} e^{(\alpha_3-\alpha_2)(x_2+w_1)} \left[-\alpha_3 Ln_3 e^{-\alpha_3(x_2+W)} + \frac{\left(\alpha_3 Ln_3 - \frac{Sn_3 Ln_3}{Dn_3}\right) e^{-\alpha_3 x_3} + \left(\frac{Sn_3 Ln_3}{Dn_3}\cosh\left(\frac{x_3-(x_2+w)}{Ln_3}\right) + \sinh\left(\frac{x_3-(x_2+w)}{Ln_3}\right)\right) e^{-\alpha_3(x_2+w)}}{\frac{Sn_3 Ln_3}{Dn_3} sinh(\frac{x_3-(x_2+w)}{Ln_3}) + \cosh(\frac{x_3-(x_2+w)}{Ln_3})} \right] \quad (12)$$

The internal quantum efficiency of the homojunction CdS(n)/CuInSe$_2$ (n)/CuInSe$_2$(p) is:

$$\eta_1 = \eta p_1 + \eta p_2 + \eta_{zce1} + \eta n_3 \quad (13)$$

2.2. Homojunction deposed on substrat CuInSe$_2$(n)/CuInSe$_2$(p)/CdTe(p)

2.2.1. Modeling

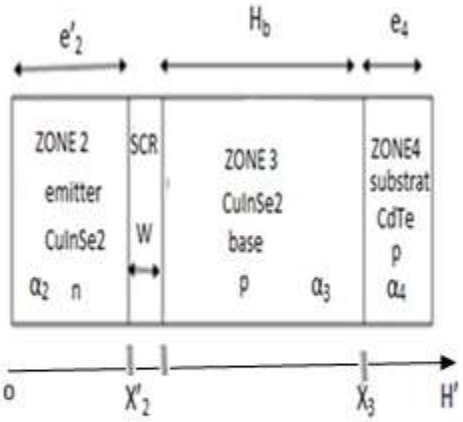

Fig 3 Diagram of the structure CuInSe$_2$ (n)/CuInSe$_2$ (p)/ CdTe (p)

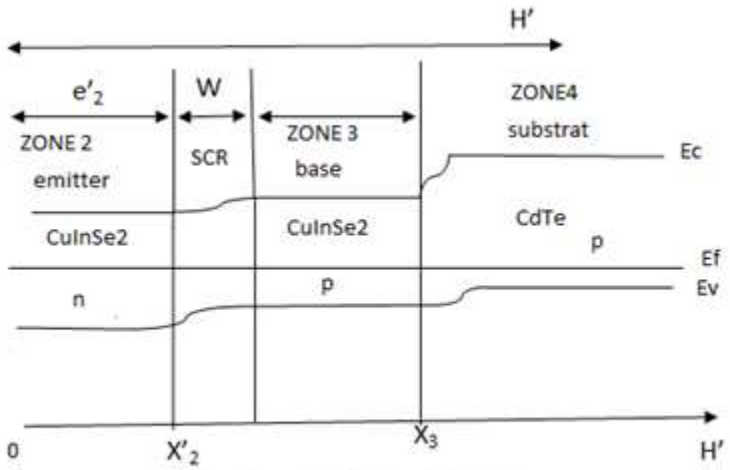

Fig 4 Energy band diagram of the structure CuInSe$_2$ (n)/CuInSe$_2$ (p)/CdTe(p)

2.2.2 Internal Quantum Efficiency in the base zone 3

The internal quantum efficiency of the emitter is the same as that of the window layer in the previous model (**2.1.2)** ($\eta p_1(x_1 = x'_2) = \eta' p_2$) you just have to replace x_1 by x'_2, L_{p1} by L'_{p2} (L'_{p2} is the diffusion length in the emitter layer), S_{p1} by S'_{p2} (S'_{p2} is the surface recombination velocity at interface window/emitter, D_{p1} by D'_{p2} (D'_{p2} is the diffusion coefficient of the holes in the zone 2 of holes) α_1 by α_2. Here only the spectral response of the base (zone3) change .In this case the continuity equations [9] governing the variation of the electrons in the base (zone3) and the substrate (zone4) are given respectively by:

$$\frac{\partial^2 \Delta n_3}{\partial^2 x} - \frac{\Delta n_3}{Ln_3^2} + \frac{\alpha_3 N(1-R)}{Dn_3} e^{(\alpha_3-\alpha_2)(x'_2+w)} e^{-\alpha_3 x} = 0 \quad (14)$$

$$\frac{\partial^2 \Delta n_4}{\partial^2 x} - \frac{\Delta n_4}{Ln_4^2} + \frac{\alpha_4 N(1-R)}{Dn_4} e^{-(\alpha_2-\alpha_3)(x'_2+w_1)} e^{-(\alpha_3-\alpha_4)x_3} e^{-\alpha_4 x} = 0 \quad (15)$$

The boundary conditions [10] are given by:

$$\Delta n_3 = 0 \qquad x = x'_2 + w_1 + w_2$$

$$Dn_3 \frac{\partial \Delta n_3}{\partial x} = Dn_4 \frac{\partial \Delta n_4}{\partial x} \qquad x = x_3 \qquad (16)$$

$$\Delta n_3 = \Delta n_4 \qquad x = x_3$$

$$\Delta n_4 = 0 \qquad x = H'$$

The internal quantum of the base is :

$$\eta' n_3 = \frac{\alpha_3 Ln_3}{\alpha_3^2 Ln_3^2 - 1}\left[-\alpha_3 Ln_3 e^{-\alpha_3 (x'_2 + w)} + Re^{-\alpha_3 x_3} + Qe^{-\alpha_3 (x'_2 + w)}\right] \qquad (17)$$

With $R = \dfrac{\left(\frac{\alpha_3 Ln_3}{b} - 1\right) + \left(1 - \frac{Dn_4 \alpha_4 Ln_3}{b Dn_3}\right)\frac{(\alpha_3^2 Ln_3^2 - 1)\alpha_4 Ln_4}{(\alpha_4^2 Ln_4^2 - 1) b \alpha_3 Ln_3}}{sinh\left(\frac{x_3 - (x'_2 + w)}{Ln_3}\right) + \frac{1}{b} cosh\left(\frac{x_3 - (x'_2 + w)}{Ln_3}\right)}$

$$Q = \frac{\frac{1}{b}\sinh\left(\frac{x_3 - (x'_2 + w)}{Ln_3}\right) + \cosh\left(\frac{x_3 - (x'_2 + w)}{Ln_3}\right)}{\sinh\left(\frac{x_3 - (x'_2 + w)}{Ln_3}\right) + \frac{1}{b}\cosh\left(\frac{x_3 - (x'_2 + w)}{Ln_3}\right)} \quad \text{and} \quad b = \frac{Dn_4 Ln_4}{Dn_3 Ln_3}$$

2.2.3. Internal quantum efficiency of space charge region [10]

$$\eta_{zce2} = (1 - e^{-\alpha_2 W}) e^{-\alpha_2 x_2} \qquad (18)$$

The sum of the internal quantum efficiency of the emitter, the space charge region and the base of the mode $CuInSe_2$ (n)/$CuInSe_2$(p)/ CdTe (p) :

$$\eta_2 = \eta p_1 (x_1 = x'_2) + \eta_{zce2} + \eta' n_3 \text{ with } \eta p_1 (x_1 = x'_2) = \eta' p_2 \qquad (19)$$

2.3. Homojunction with window and deposed on substrat CdS(n)/$CuInSe_2$(n)/$CuInSe_2$(p)/CdTe(p).

2.3.1 . Modeling

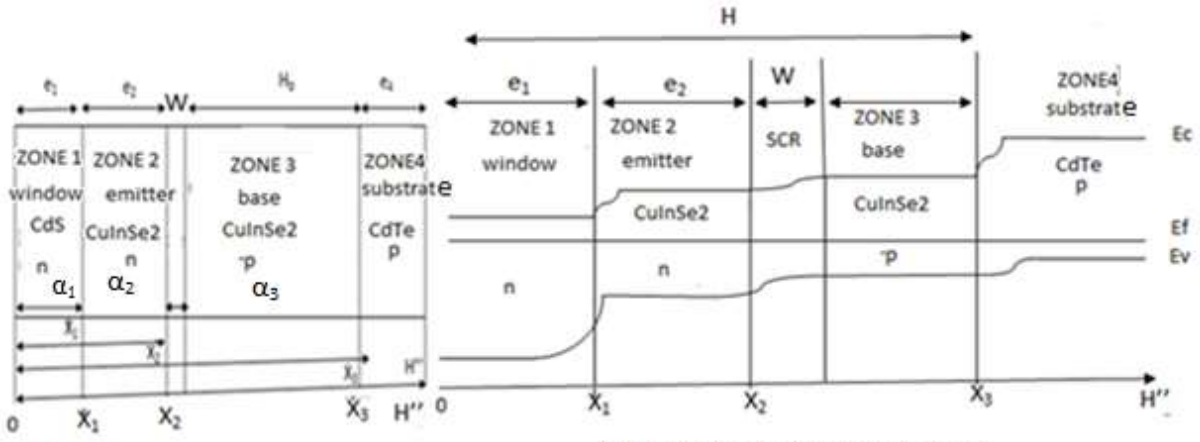

Fig 5: Diagram of the structure CdS(n)/$CuInSe_2$(n)/ $CuInSe_2$(p)/CdTe(p)

Fig 6: Energy band diagram of the structure CdS(n)/$CuInSe_2$(n)/ $CuInSe_2$(p)/CdTe(p)

2.3.2. Internal Quantum Efficiency of the base (zone3)

The internal quantum efficiency contribution of the window layer (zone 1) of the emitter layer (zone2) and the region of space charge is the same as that of the homojunction with window CdS(n)/$CuInSe_2$(n)/$CuInSe_2$(p) studied

in (2.1.2; 2.1.3 ;2.1.4). However we note a change due to a term from the window layer of the internal quantum efficiency of the base ($\eta'n_3$).The continuity equations of the base and substrate are respectively given by[9]

$$\frac{\partial^2 \Delta n_3}{\partial^2 x} - \frac{\Delta n_3}{Ln_3^2} + \frac{\alpha_3 N(1-R)}{Dn_3} e^{-x_1(\alpha_2-\alpha_1)} e^{(\alpha_2-\alpha_3)(x_2+w)} e^{-\alpha_3 x} = 0 \quad (20)$$

$$\frac{\partial^2 \Delta n_4}{\partial^2 x} - \frac{\Delta n_4}{Ln_4^2} + \frac{\alpha_4 N(1-R)}{Dn_4} e^{-x_1(\alpha_2-\alpha_1)} e^{-(\alpha_2-\alpha_3)(x_3+w)} e^{(\alpha_3-\alpha_4)x_3} e^{-\alpha_4 x} = 0 \quad (21)$$

α_4 absorption coefficient of CdTe, D_{n4} is diffusion coefficient of the electrons in the substrate , L_{n4} is the diffusion lenght of the electrons in the substrat. The variation of electrons in the base and the substrate are given by the following equations:

$$\Delta''n_3 = A''exp\left(\frac{x}{Ln_3}\right) + B''exp\left(-\frac{x}{Ln_3}\right) + K''_3 e^{-\alpha_3 x} \quad (22)$$

$$\Delta''n_4 = M''exp\left(\frac{x}{Ln_4}\right) + N''exp\left(-\frac{x}{Ln_4}\right) + K''_4 e^{-\alpha_4 x} \quad (23)$$

$K''_3 = \frac{\alpha_3 N(1-R)Ln_3^2}{Dn_3(\alpha_3^2 Ln_3^2-1)} e^{-x_1(\alpha_2-\alpha_1)} e^{(\alpha_3-\alpha_2)(x_2+w)}$; $K''_4 = \frac{\alpha_4 N(1-R)Ln_4^2}{Dn_4(\alpha_4^2 Ln_4^2-1)} e^{-x_1(\alpha_2-\alpha_1)} e^{(\alpha_3-\alpha_2)(x_2+w)}$

The boundary conditions [10] are given by:

$$\begin{aligned} &\Delta n_3 = 0 && x = x_2 + w_1 + w_2 \\ &Dn_3 \frac{\partial \Delta n_3}{\partial x} = Dn_4 \frac{\partial \Delta n_4}{\partial x} && x = x_3 \\ &\Delta n_3 = \Delta n_4 && x = x_3 \\ &\Delta n_4 = 0 && x = H'' \end{aligned} \quad (24)$$

The internal quantum efficiency of the base of the homojunction with window and deposited on substrate is :

$$\eta''n_3 = \frac{\alpha_3 Ln_3}{\alpha_3^2 Ln_3^2-1} e^{-x_1(\alpha_2-\alpha_1)} e^{-\alpha_3(x_2+w)} [-\alpha_3 Ln_3 + Te^{-\alpha_3(x_3-(x_2+w)+V}] \quad (25)$$

with $T = \frac{[-b + \frac{1}{(\alpha_4^2 Ln_4^2-1}\left(\alpha_3 Ln_3 + \frac{\alpha_4 Ln_4}{\alpha_3 Ln_3}\right)]}{b\sinh\left(\frac{x_3-(x_2+w)}{Ln_3}\right)+\cosh\left(\frac{x_3-(x_2+w)}{Ln_3}\right)}$ and V = $\frac{\sinh\left(\frac{x_3-(x_2+w)}{Ln_3}\right)+b\cosh\left(\frac{x_3-(x_2+w)}{Ln_3}\right)}{b\sinh\left(\frac{x_3-(x_2+w)}{Ln_3}\right)+\cosh\left(\frac{x_3-(x_2+w)}{Ln_3}\right)}$

The sum of the internal quantum efficiency contributions of the four regions of the CdS (n) / $CuInSe_2$ (n) / $CuInSe_2$ (p) /CdTe (p) homojunction is given by the following equation:

$$\eta_3 = \eta''p_1 + \eta''p_2 + \eta_{zce3} + \eta''n_3 \quad (26)$$

With $\eta''p_1 = \eta p_1$, $\eta''p_2 = \eta p_2$ and $\eta zce_1 = \eta zce_3$

RESULTATS AND DISCUSSION

In this work we study the spectral reponses versus the energy of photon of the different solar cells with the following materials $CuInSe_2$ CdTe and CdS function of the energy of the photons.The varaiation of the absorption coefficients of these materials according to the energy of the photons is given by the following figure1[1]

ISSN: 2277-9655
Impact Factor: 4.116

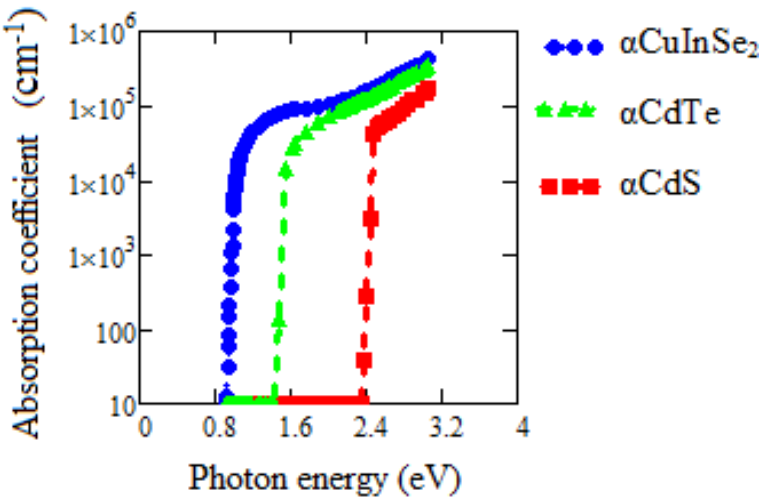

Figure7: Absorption coefficient of $CuInSe_2$ CdTe and CdS vs photons energy

1. **Comparaison the three models of homojunction**

1.1. Internal quantum efficiency of the emitters, bases and space charge zones of the different cells studied

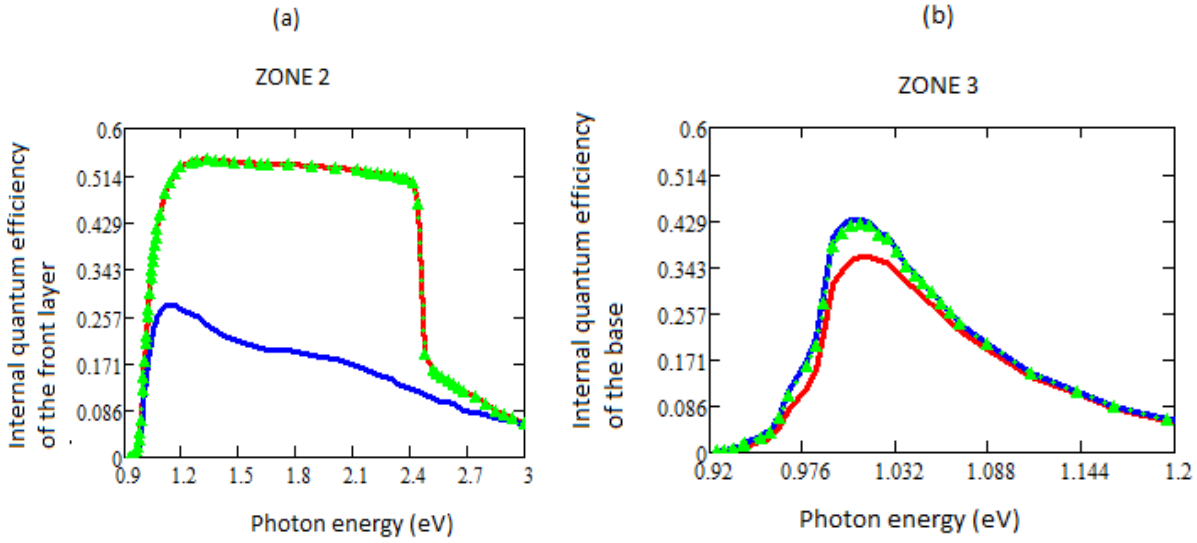

ISSN: 2277-9655
Impact Factor: 4.116

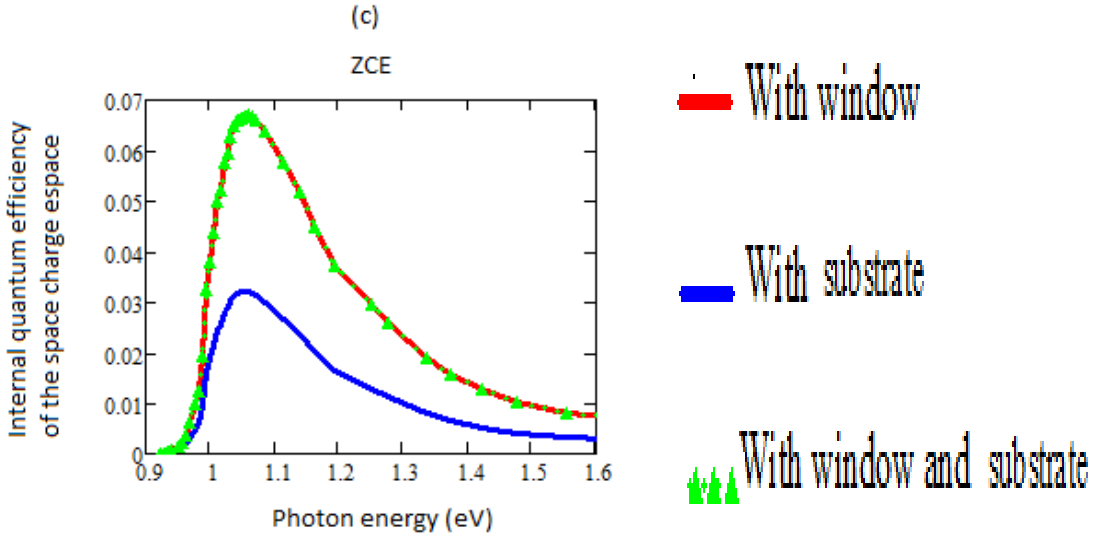

Figure8: Internal Quantum Efficiency vs photons energy

a) Contribution of the different emitter layers b) contribution of the different base c) Contribution of the different space charge region

Zone2: emitter layer

With window

$Sp_1 = 2.10^7 cm/s$, $x_1 = 0{,}5\mu m$, $Dp_1 = 20cm^2/s$, $Lp_1 = 0{,}5\mu m$, $Sp_2 = 2.10^5 cm/s$, $Lp_2 = 0{,}5\ \mu m$ $Dp_2 = 20cm^2/s$ $x_2 = 1\mu m$, $e_2 = 0{,}5\mu m$.

With substrate we have used the same values of parameters that window ($L'p_2 = Lp_2$, $D'p_2 = Dp_2$, $e_2 = x'_2$).

With substrate $S'p_2 = 2.10^7 cm/s$

with window and substrate we have used the same value of the parameters Sp_1, x_1, x_2, e_2, Lp_1, Sp_2, Lp_2 that the model with window.

Space charge region (scr)

With window: , $W = W_1 + W_2 = 0{,}1\mu m$

For the model with substrate and with window and deposed on substrat we have used the same values of parameter that **with window :**

Zone3 :base

With window:

$x_1 = 0{,}5\mu m$ $x_2 = 1\mu m$ $e_2 = x_2 - x_1 = 0{,}5\mu m$; $Sn_3 = 2.10^6 cm/s$, $Ln_3 = 3\mu m$,

, $Dn_3 = 20cm^2/s$, $W = W_1 + W_2 = 0{,}1\mu m$, $H_b = 2{,}9\mu m$

With substrate

$Dn_4 = 20cm^2/s$, $Ln_4 = 3\mu m$

With window and substrate:

We have used the same values of x_1, x_2, Sn_3, Ln_3, W, H_b, Dn_3, Dn_4 and Ln_4 that the model with window and with substrate (for the model with substarte and with window deposed in substrate).

In this work,we study the internal quantum efficiency of different solar cells models as a function of photon energy. We find an improvement in the internal quantum efficiency of the emitters of the following homojunction: CdS (n) / $CuInSe_2$ (n) / $CuInSe_2$ (n) / $CuInSe_2$ (n)/$CuInSe_2$ (p) / CdTe (p). These two internal quantum efficiency are equal and are of the order of 54.3% (Fig.8a). Quantum efficiency is due to the reduction of surface losses. The internal quantum efficiency of homojunction deposited on a CdTe: $CuInSe_2$ (n) / $CuInSe_2$ (n)/ CdTe (p) substrate is much lower compared to the other two models (22% Fig.8a). The range of energies between 0.92 eV and 1.05 eV

corresponds to the absorption of $CuInSe_2$ which generates carriers which will be collected if thediffusion lengths are in order of the width ($Lp_1 = e_1; Lp_2 = e_2;$ $Ln_3 = Hb$) and gives a internal quantum efficiency of 54.3%. The window layer limits the number of photons arriving at the active region . This justifies the fall in internal quantum efficiency for energies greater or equal to 2.4 eV.

At the figure 8b, the internal quantum effieciency of homojunctions of $CuInSe_2$ (n) / $CuInSe_2$ (p) / CdTe (p) and CdS (n) / $CuInSe_2$ (n) / $CuInSe_2$ (p) CdTe (p) is greater than that of the CdS (n) / $CuInSe_2$ (n) / $CuInSe_2$ (p) model. The internal quantum efficiency of the first two remain equal and give 41.2%. We affirm that the effect of the substrate is at the origin of this difference.

The internal quantum efficiency of the CdS (n) / $CuInSe_2$ (n) / $CuInSe_2$ (p) and CdS (n) / $CuInSe_2$ (n) / $CuInSe_2$ CdTe (p) is of the same order of magnitude and is 6.7% higher than that of the $CuInSe_2$ (n) / $CuInSe_2$ (p) / CdTe (p) mode.

1.2. Comparaison of the internal quantum efficiency of the homojunctions : CdS(n)/$CuInSe_2$(n)/$CuInSe_2$(p);$CuInSe_2$(n)/$CuInSe_2$(p) /CdTe(p);CdS(n)/$CuInSe_2$(n)/$CuInSe_2$(p) /CdTe(p),,

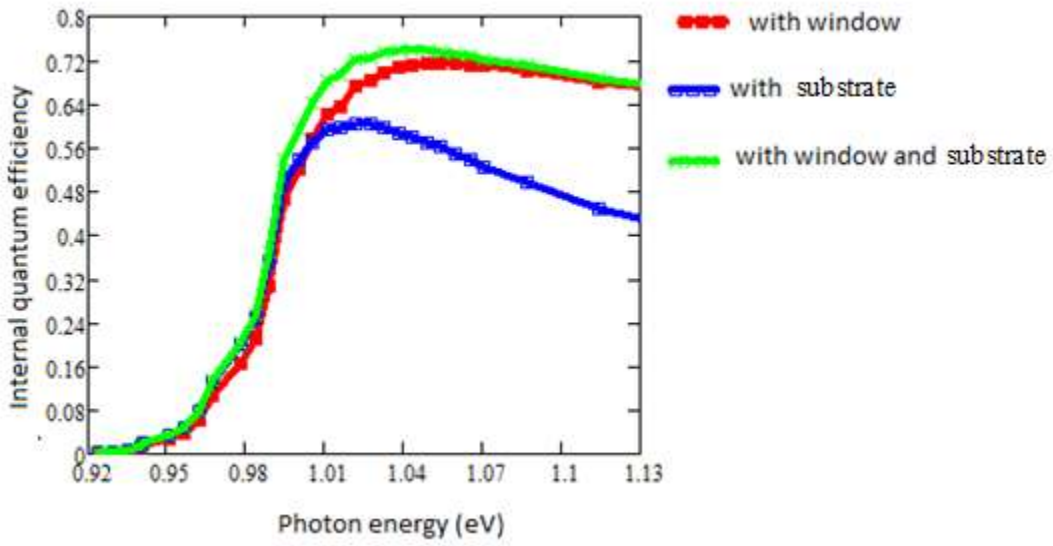

Figure 9: Internal Quantum Efficiency contribution of the different models

CdS(n)/$CuInSe_2$(n)/$CuInSe_2$(p),:
$Sp_1 = 2.10^7 cm/s$, $x_1 = 0{,}5\mu m$, $Dp_1 = 20cm^2/s$, $Lp_1 = 0{,}5\mu m$, $Sp_2 = 2.10^5 cm/s$, $Lp_2 = 0{,}5\ \mu m$ $Dp_2 = 20cm^2/s$ $x_2 = 1\mu m$ $e_2 = x_2 - x_1$ $Sn_3 = 2.10^6 cm/s$, $Ln_3 = 3\mu m$ $Dn_3 = 20cm^2/s$ $W = W_1 + W_2 = 0{,}1\mu m$ $H_b = 2{,}9\mu m$;

$CuInSe_2$(n)/$CuInSe_2$(p)/CdTe(p):
$L'p_2 = Lp_2$,$D'p_2 = Dp_2$, $e_2 = x'_2$; Sn_3, Ln_3, Dn_3 ; w, that the model with window, $S'p_2 = 2.10^7 cm/s$, $Dn_4 = 20cm^2/s$ $Ln_4 = 3\mu m$.

CdS(n) /$CuInSe_2$(n)/$CuInSe_2$(p)/CdTe (p)
We have used the same values of Sp_1 , x_1 , Dp_1, Lp_1, x_2 , e_2 , Sp_2 , Lp_2 , Dp_2, Sn_3, Ln_3, Dn_3, W, H_b , Ln_4 , Dn_4 that the model with window.

The three curves of figure 9 represent the variations of the internal quantum efficiency for the different devices: CdS (n) / $CuInSe_2$ (n)/ $CuInSe_2$ (p) , $CuInSe_2$ (n)/ $CuInSe_2$ (p)/ CdTe (p) and CdS (n) / $CuInSe_2$ (n) / $CuInSe_2$ (p) / CdTe (p). The photons whose energies are greater than the gap of the $CuInSe_2$ generate the carriers which are collected under the effect of the internal electric field if they reach the space charge region .This explains the increase in internal quantum efficiency for energies between 0.924 eV and 1.05 eV. When the energy of the photons

is greater than 1.05 eV, the generation rate which was 42.9% passes to 11.4% for an energy photon of 1.2 eV with a thickness e_2 = 0.5 µm. This justifies the decrease of the internal quantum efficiency. The CdS (n) / $CuInSe_2$ (n) / $CuInSe_2$ (p) / CdTe (p) model gives the best internal quantum efficiency which is of the order of 73.8% with an emitter thickness of e_2 = 0.5µm, a surface recombination velocity at the window of $Sp_2 = 2.10^5$ cm / s and a diffusion length of the electrons of Lp_2 = 0.5 µm. This model combines the two advantages obtained with the window layer CdS (n) and the substrate CdTe (p). The window layer reduce the losses at the surface of the buffer layer [4]. The substrate create a junction presenting an electric field which return the carriers which are not normally collected. In order to maximize the internal quantum efficiency, we have taken $Lp_1 = e_1$ = 0,5µm and $Lp_2 = e_2$ = 0,5µm.

1.3. Homojunction with window deposited on substrate: CdS(n) /$CuInSe_2$(n)/$CuInSe_2$(p)/CdTe(p)

1.3.1 Window layer (zone 1) : Effect of thickness (e_1) , diffusion length (L_{p1}) and recombination velocity (Sp_1)

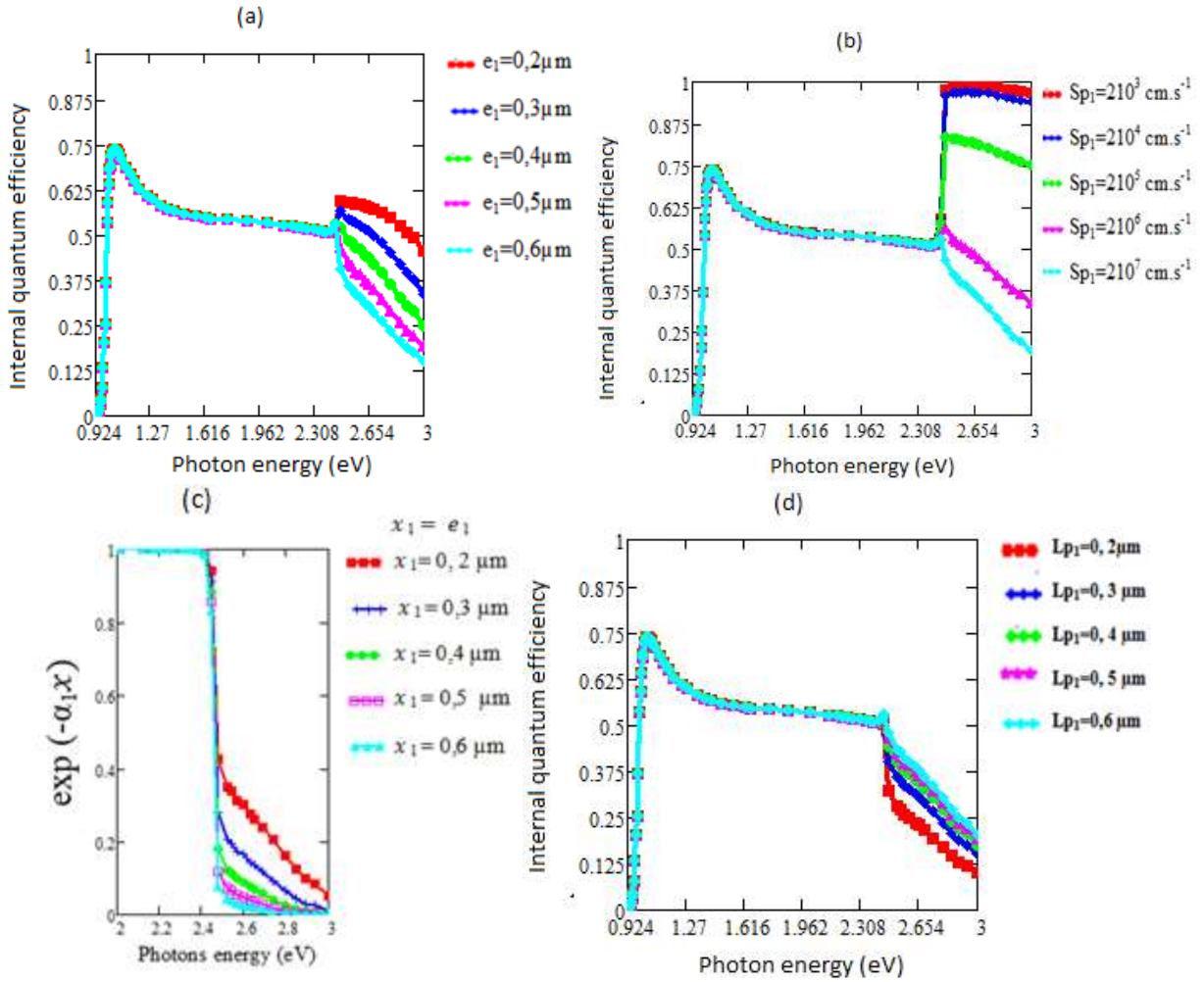

Thickness of window layer (µm)	Photons energy / génération rate		
e_1=0,2	2,45eV/85,7%	2,5 eV /37,5%	2,6 eV /30%
e_1=0,3	2,45 eV/77,8%	2,5 eV /25%	2,6 eV /17,5%
e_1=0,4	2,45 eV /75%	2,5 eV /11,3%	2,6 eV /8,8%
e_1=0,5	2,45 eV /72%	2,5 eV /10%	2,6 eV /5%
e_1=0,6	2,45 eV/71,4%	2,5 eV /5,7%	2,6 eV /2,5%

Table 2: Rate of generation of the carriers according to the energy of the photons for various values ' thicknesses of the window

Figure 10: Internal Quantum Efficiency vs. photons energy for different.

a)Effect of the window thickness

$Sp_1 = 2.10^7 cm/s$; $Dp_1 = 20cm^2/s$; $Lp_1 = 0,5\mu m$; $Sp_2 = 2.10^5 cm/s$ $Lp_2 =$ 0,5 µm; $Dp_2 = 20cm^2/s$; $x_2 = 1\mu m$; $e_2 = x_2 - x_1$; $S_{n3} = 2.10^6 cm$ /1 , $Ln_3 = 3\mu m$, $Dn_3 = 20cm^2/s$, $W = W_1 + W_2 = 0,1\mu m$; $H_b = 2,9\mu m$; $Dn_4 = 20cm^2/s$, $Ln_4 = 3\mu m$.

b) Effect of the recombination velocity on the window surface.

c) Rate of generation of the carriers according to the energy of the photons for various values ' thicknesses of the window.

d) Effect of the diffusion length of the holes in the zone1 . We have used the same value of a)

The CdS constitutes the window layer of the homojunction and is transparent. This transparence [12] depends on the thickness of the CdS. This is why we study the behavior of the cell as a function of the thickness of CdS layer [13] Fig. 10a. The energy range from 0.924 eV to 2.4 eV (for Fig. 10a, 10b, 10d) corresponds to the absorption of the emitter and $CuInSe_2$ base (n /p). The front and base $CuInSe_2$ (n/p) have a energy of gap (0.924 eV) .The window layer (2.4 eV) will absorb at the first. This absorption generates charge carriers which contribute to the photocurrent. Photons energies greater than 2.4eV are absorbed by the window layer.On Figure 10a, the increase of window thickness decreases the rate generation of the carriers in this region and the absorption of photons in the emitter and in the base [14]. This explains the decrease of the internal quantum efficiency with the increase of this thickness (60% with 0.2 µm to 50% with 0.6 µm). Indeed for an energy of 2.45eV, the generation rate for different thicknesses decreases (85.7% for e_1 = 0.2µm, 71.4% for e_1 = 0.6µm). for the same photon energy of 2.5eV we also have the following proportions: (37.5% for e_1 = 0.2µm, 5.7% for e_1 = 0.6µm) see Table 2. The decrease of the generation rate also justifies the drop of internal quantum efficiency.

The surface recombination velocity(Sp_1) shows the hanging links and the high concentrations of the impurities linked to the doping [15]. However, this recombination velocity can be reduced by depositing an antireflection layer on the surface of the CdS material [15].At the figure10b, for the energies greater than 2.4ev the internal quantum efficiency decreases with the increase of the rate of recombination. When the defects are important some carriers are lost and the spectral response decreases gradually. The highest quantum efficiency is obtained with the lowest recombination velocity (99% with $Sp_1 = 2.10^3$ cm/s). The internal quantum efficiency passes to 99% with $Sp_1 = 2.10^2$ cm /s to 50% with $Sp_1 = 2.10^7 cm$ /s. We observe the best internal quantum efficiency (99%) with energies higher than 2.4eV because the photons are absorbed by the window layers and do not reach the emitter and the base.

The diffusion lengths (Lp_1) depend on the technology in particular of the methods used for the doping and the creation of the junction.]. At the figure 10d, the internal quantum efficiency increases with the diffusion length of the holes in the window layer . Some carriers have the necessary time to reach the junction and will be collected. For the diffusion lengths whose are greater than or equal to the thickness of the front layer ($Lp_1 = 0,5\mu m ; 0,6\mu m, ; 0,7\mu m \geq e_1 = 0,5\mu m$) the spectral response hardly varies. The holes have time to reach the space charge region.

ISSN: 2277-9655
Impact Factor: 4.116

1.3.2. Emitter layer (zone2) : Effect of thickness (e_2) , diffusion length (L_{p2}) and recombination velocity (Sp_2)

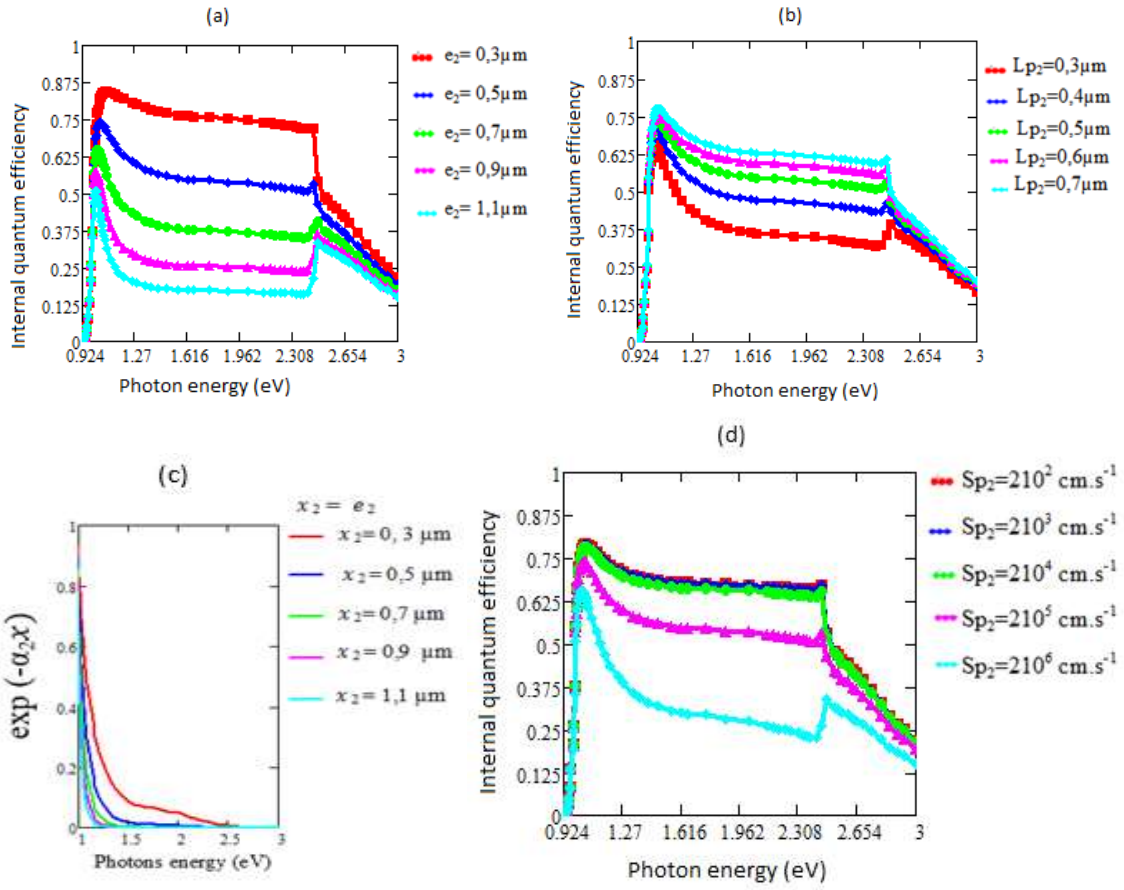

Thickness of window layer (µm)	Photons energy / génération rate (%)/		
e_2=0,3	1,05eV/60%	1,2eV /25,7%	1,5eV /8,6%
e_2=0,5	1,05eV/42,9%	1,2eV /11,4%	1,5eV /1,71%
e_2=0,7	1,05eV /28,6%	1,2eV /4,3%	1,5eV /0,35%
e_2=0,9	1,05eV /20,8%	1,2eV /1,67%	1,5eV /0,06%
e_2=1,1	1,05eV/16%	1,2eV /0,6%	1,5eV /0,02%

Table3: Rate of generation of the carriers according to the energy of the photons for various values ' thicknesses of the emitter

Figure 11: Internal Quantum Efficiency vs photons energy

a) Effect of the thickness emitter

$Sp_1 = 2.10^7 cm/s$, $Dp_1 = 20cm^2/s$; $Lp_1 = 0,5\mu m$, $Sp_2 = 2.10^5 cm/s$, $Lp_2 = 0,5\ \mu m$ $Dp_2 = 20cm^2/s$ s; $Sn_3 = 2.10^6 cm/s$, $Ln_3 = 3\mu m$; $Dn_3 = 20cm^2/s$; $W = W_1 + W_2 = 0,1\mu m$, $H_b = 2,9\mu m$; $Dn_4 = 20cm^2/s$; $Ln_4 = 3\mu m$.

b)Effect of the diffusion length of holes in the emitter.

c) Rate of generation of the carriers according to the energy of the photons for various values ' thicknesses of the emitter.
d) Effect of the recombination velocity at interface window-emitter.
We have used the same values that a) for b) ;c) and d)

Our aim is to reduce the recombination velocity at the surface of the emitter $CuInSe_2$ (n). We propose a deposit of CdS on its surface. However, the thickness of this layer remains an indispensable parameter for obtaining a good internal quantum efficiency. That is the reason to study its influence on internal quantum efficiency. The energy range between 0.924 eV and 2.4 eV corresponds to the absorption of the $CuInSe_2$ (n) emitter and the $CuInSe_2$ (p) base. For Fig.11a, the internal quantum efficiency decreases with the increase the thickness of the emitter. We obtain a better internal quantum efficiency of 84.5% with a thickness of 0.3µm. When the width of the front is low the carriers are generated just at the junction and therefore will participate to the photocurrent.When the thickness increases, the carries are generated just at junction and some carriers whose diffusion lengths are less than this thickness will be lost (Lp_2 = 0,5µm < e_2 = 0 ,7µm ; 0 ,9µm ; 1 ,1µm). This attenuates the internal quantum efficiency and goes from 84.5% for e_2 = 0.3 µm to 50.6% with e_2 = 1.1 µm. We notice a reduction of the generation rate with the increase in thickness. Indeed, for an energy of 1.05 eV , the generation rate for differents thickness passe: (60% for e_2 = 0.3 µm, 16% for e_2 = 1.1 µm). For the same photon of energy of 1.2eV, we also have the following proportions: 25.7% for e_2 = 0.3µm and 0.6% for e_2 = 1.1 µm .At the figure 11b, the internal quantum efficiency increases with the diffusion length of the electrons in the emitter because some carriers will have the time necessary to reach the junction and will be collected. Those for which the diffusion lengths are greater than or equal to the thickness of the frontal layer ($Lp_2 = 0,5\mu m; 0,6\mu m; 0,7\mu m$) the spectral response hardly do not varies and reaches 78% with a diffusion length of 0.7 µm.
The electrons have already a sufficient diffusion length to reach the space charge area ($Lp_2 = 0,5\mu m; 0,6\mu m; 0,7\mu m \geq e_2 = 0,5\ \mu m$).
The surface recombination velocity (Sp_2) at the window/emitter interface ($CdS/CuInSe_2$) shows the compatibility between the parameters of the materials. More it has defects in this zone , more the probability of collecting the carriers is lower, consequently the photocurrent decreases gradually. At the figure 11d , the internal quantum efficiency decreases when the defects become larger .We notice a limit surface recombination velocity
($Sp_2 = 2.10^3$ cm /s) below which the internal quantum efficiency (78.8%) dot not varies.

CONCLUSION

In this work we have established the expressions of the internal quantum efficiency of each model. We have plotted the variations of these internal quantum efficiency as a function of the photon energies. These variations allowed us to choose the model giving the best internal quantum efficiency. With this model we have studied the influence of the thicknesses of the window layer and the emitter, the surface recombination velocity at the window/emitter interface (Sp_2) , the diffusion lengths of the carriers in the emitter and the window layer (Lp_1, Lp_2) of homojunction with window and deposited on substrate (CdS (n) / $CuInSe_2$ (n) / $CuInSe_2$ (p) / CdTe (p)). The comparative study of the models permit to conclude that the homojunction with window and deposited on the substrate provides an ideal internal quantum efficiency of 73.8%.We also find that the effect of the window dominates the effect of the substrate. The effect of the substrate is sensitive by increasing the diffusion length of the electrons in the base and in the substrate. In order to obtain optimum internal quantum efficiency, it is necessary to choose a small emitter thickness ($e_2 = 0.5$ µm), a low surface recombination velocity ($Sp_1 \leq 2.10^4$ cm / s) and at window/emitter interface ($Sp_2 \leq 2.10^3$ cm / s. The diffusion lengths of the holes and the electrons must be greater than or equal to the width of the buffer layer and the base ($Lp_2 \geq 0.5\mu m$ and $Ln_3 \geq 3\mu m$). It is important to choose a window layer and a substrate whose lattice matched are close to that of the base material which is $CuInSe_2$. This will reduce the loss of interfaces to improve internal quantum efficiency.

.

ISSN: 2277-9655
Impact Factor: 4.116

REFERENCES

1. Linda SAAD HAMIDECHE «Etude des propriétés du matériau ternaire $CuInSe_2$ à base de Cu de la famille des chalcopyrites Cu-III-VI2 » Thèse de doctorat Université Badji Mokhtar Anna 2012 pp 12- 26.
2. T. Wada, H. Kinoshita, Thin Solid Films 480–481 (2005) 92–94.
3. BOUAFIA MOUNIR DEBLAOUI LAI «Modélisation et simulation d'une cellule solaire en couche mince à base de di séléniure de Cuivre, d'Indium et de Gallium CIGS» Mémoire de Master professionnel. Université Kasdi Merbah–Ouargla 2012 pp 32.
4. Aurélien DUCHATELET, « Synthèse de couches minces de Cu (In, Ga) Se_2 pour cellules solaires, par électro-dépôt d'oxydes mixtes de cuivre-indium-gallium » Thèse de doctorat . UNIVERSITE LILLE1 (France), 2012 pp 22
5. E.M. Keita*, B. Mbow, M.S. Mane, M.L. Sow, C. Sow, C. Sene '' Theoretical Study of Spectral Responses of Homojonctions²2Z Based on $CuInSe_2$''Journal of Materials Science & Surface Engineering Vol. 4 (4), 2016, pp 392-399.
6. HAROUNI SOFIANE, «Etude optique de la déformation dans quelques semi-conducteurs II-VI» Thèse de doctorat .UNIVERSITE MENTOURI CONSTANTINE (Algérie), 2007 pp 11.
7. Mme BENGHABRIT Siham, « Elaboration et caractérisation de couches minces CdS par bain chimique CBD pour application photovoltaïque» Thèse de doctorat .Université des Sciences et de la Technologie d'Oran« Mohamed BOUDIAF **»** (Algérie), 2015 pp 40.
8. S.Madougou[1,a+] ,F.Made[2,b] ,M.Boukary[3,c] and G. Sissoko[4,d] Recombination parameters Determination by Using Internal Quantum Effiency (IQE) Data on Bifacial Silicon Solar Cells ,Advanced Materials Research Vols. 18-19 (August 2007) pp. 314.
9. E.M. Keita*, B. Mbow , M.L. Sow, C. Sow, M. Thiam ''theorical comparative study of internal quantum efficiency of thin films solar cells based on $CuInSe_2$: p+/p/n/n+, p/n/n+, p+/p/n and p/n models'' International Journal of Engineering Science & Research Technology Vol. 5 (9), 2016, pp 347-399.
10. B.MBOW, A.MEZERREG, N.REZZOUG and C.LLINARE 'Calculed and measure spectral response in near-infrarouge of III-V photo detectors based on Ga ,In and Sb' Physica Status Solidi (a) (1994) pp 513-514-515-517-520-523-524.
11. A.LAUGIER U. A. Roger, « Les photopiles solaires, Technique et Documentation», Ed 1981 pp 110.
12. V.P. Singh, D.L. Linam, D.W. Dils, J.C. McClure and G.B. Lush, '*Electro-Optical Characterization and Modeling of Thin Film CdS-CdTe Heterojunction Solar Cells*', SolarEnergy Materials and Solar Cells, Vol. 63, N°4, pp. 445 – 466, 2000.
13. O.A. Niasse[1]*, B. Mbengue[1], B. BA[1], A. Ndiaye[1] et I. Youm[1] 'Effets des excitons sur le rendement quantique de la cellule solaire CdS/CdTe par le modèle de la fonction diélectrique' *Revue des Energies Renouvelables Vol. 12 N°3 (2009) 503* .
14. N. Touafek, M.S. Aida, R.Mahamdi « $CuInSe_2$ Solar Cells Efficiency Optimization » America Journal of Materials Science 2012,2(5) pp 160-164.
15. Anne Kaminski[1], Mathieu Monville Cours « Energie photovoltaïque :Physique des composants nanostructures», [1]INP Grenoble –INSA Lyon [2]Solarforce PHELMA-Septembre 2010 pp 22 .